



Low thermal conductivity of the negative thermal expansion material, Hf Mo 2 O 8

Catherine A. Kennedy, Mary Anne White, Angus P. Wilkinson, and Tamas Varga

Citation: [Applied Physics Letters](#) **90**, 151906 (2007); doi: 10.1063/1.2721860

View online: <http://dx.doi.org/10.1063/1.2721860>

View Table of Contents: <http://scitation.aip.org/content/aip/journal/apl/90/15?ver=pdfcov>

Published by the [AIP Publishing](#)

Articles you may be interested in

[First-principles study of negative thermal expansion in zinc oxide](#)

J. Appl. Phys. **114**, 063508 (2013); 10.1063/1.4817902

[Measurement of anharmonicity of phonons in the negative thermal expansion compound Zn \(CN \) 2 by high pressure inelastic neutron scattering](#)

Appl. Phys. Lett. **95**, 201901 (2009); 10.1063/1.3264963

[Lattice thermal conductivity of graphene flakes: Comparison with bulk graphite](#)

Appl. Phys. Lett. **94**, 203103 (2009); 10.1063/1.3136860

[Thermal expansion and Gruneisen parameters in some Pr–Ni–Si compounds](#)

J. Appl. Phys. **97**, 10M516 (2005); 10.1063/1.1853894

[Thermal conductivity of germanium, silicon, and carbon nitrides](#)

Appl. Phys. Lett. **81**, 5126 (2002); 10.1063/1.1533840

The image shows the cover of an Applied Physics Reviews journal issue. It features a blue and orange color scheme with a molecular structure background. The text 'NEW Special Topic Sections' is prominently displayed in white. Below it, the text 'NOW ONLINE' is in orange, followed by 'Lithium Niobate Properties and Applications: Reviews of Emerging Trends' in white. The AIP Applied Physics Reviews logo is in the bottom right corner.

NEW Special Topic Sections

NOW ONLINE
Lithium Niobate Properties and Applications:
Reviews of Emerging Trends

AIP Applied Physics Reviews

Low thermal conductivity of the negative thermal expansion material, HfMo_2O_8

Catherine A. Kennedy and Mary Anne White^{a)}

*Department of Chemistry, Dalhousie University, Halifax, Nova Scotia B3H 4J3, Canada
and Institute for Research in Materials, Dalhousie University, Halifax, Nova Scotia B3H 4J3, Canada*

Angus P. Wilkinson

School of Chemistry and Biochemistry, Georgia Institute of Technology, Atlanta, Georgia 30332-0400

Tamas Varga

*Thermochemistry Facility, University of California at Davis, Davis, California 95616
and NEAT ORU, University of California at Davis, Davis, California 95616*

(Received 27 February 2007; accepted 12 March 2007; published online 10 April 2007)

The thermal conductivity of the cubic polymorph of hafnium molybdate, HfMo_2O_8 , was determined over the temperature range of 2–400 K. The values of thermal conductivity were low ($0.64 \pm 0.15 \text{ W m}^{-1} \text{ K}^{-1}$ at $T=300 \text{ K}$ for a fully dense sample), with a positive temperature coefficient throughout the temperature range examined. Calculations of the theoretical minimum thermal conductivity and the effective phonon mean free path show that the heat-carrying phonons are nearly fully coupled in HfMo_2O_8 , consistent with the rather large magnitude of its Grüneisen parameter. The low-frequency optic modes which lead to negative thermal expansion in HfMo_2O_8 are likely responsible for the low thermal conductivity. © 2007 American Institute of Physics.

[DOI: 10.1063/1.2721860]

Although most materials expand when heated, a surprising number exhibit the opposite behavior, sometimes over wide temperature ranges and over more than one crystallographic direction.^{1,2} Of particular interest is the family of materials of the general formula AB_2O_8 . With $A=\text{Zr}$ and $B=\text{W}$, thermal expansion is large and negative (approximately $-9 \times 10^{-6} \text{ K}^{-1}$) over the temperature range of 0.5–K to 1050 K.^{3–5} Other members of this group with negative thermal expansion include ZrMo_2O_8 , HfW_2O_8 , and HfMo_2O_8 .

On the basis that the low-frequency modes that give rise to negative thermal expansion could also influence other thermal properties, we determined the thermal conductivity of ZrW_2O_8 and found it to be very low, close to the theoretical minimum thermal conductivity.⁶ Here, we report the thermal conductivity of the cubic polymorph of hafnium molybdate, HfMo_2O_8 , which is also known to exhibit negative thermal expansion ($\alpha_T = -4.0 \times 10^{-6} \text{ K}^{-1}$ or $T=77\text{--}573 \text{ K}$).⁷

$\text{HfMo}_2\text{O}_7(\text{OH})_2 \cdot 2\text{H}_2\text{O}$ was produced by the reaction of aqueous solutions of $\text{HfCl}_2\text{O} \cdot 8\text{H}_2\text{O}$ (Alfa Aesar, Ward Hill, MA) and $(\text{NH}_4)_6\text{Mo}_7\text{O}_{24} \cdot 4\text{H}_2\text{O}$ (Strem Chemicals, Newburyport, MA) in acid medium during 3 days of refluxing. Then $\text{HfMo}_2\text{O}_7(\text{OH})_2 \cdot 2\text{H}_2\text{O}$ was dehydrated by a series of low-temperature heat treatment steps (350 °C for 12 h, 375 °C for 20 min, 400 °C for 20 min, 425 °C for 30 min, 450 °C for 30 min, 475 °C for 30 min, and, finally, an additional 30 min at 475 °C), separated by cooling to room temperature for x-ray analysis.

Thermogravimetric analysis gave a Hf:Mo mole ratio of 1:2.03. From x-ray diffraction, the content of trigonal HfMo_2O_8 was estimated to be ~0.1%. Differential scanning calorimetry from $T=300$ to 460 K indicated no thermal

anomalies and put an upper limit on water content of 0.5 mass %. To check the sample's amorphous content, laboratory powder x-ray diffraction data were collected on 70:30, 60:40, and 50:50 mass % mixtures of HfMo_2O_8 with an internal standard, Y_2O_3 . The data were analyzed using the Rietveld method to obtain mass fractions for the two major crystalline phases. The sample was estimated to be ~92% crystalline cubic HfMo_2O_8 from these mass fraction determinations.

The sample was kept under vacuum except when making pellets for thermal conductivity measurements, which required brief exposure to air. The HfMo_2O_8 powder was pressed into disk-shaped pellets with a diameter of 4.74 mm using a load of 0.5 GPa. High-pressure x-ray diffraction studies have shown that cubic HfMo_2O_8 starts to amorphize above 0.3 GPa and undergoes a phase transition between 0.7 and 2.0 GPa,⁸ but x-ray diffraction results before and after pressing of the pellets were identical.

Temperature-dependent thermal conductivities were determined using the thermal transport option of a Quantum Design Physical Properties Measurement System (PPMS, QD). A two-probe configuration (heater and hot thermometer shared one lead, while the coldfoot and cold thermometer shared the other) was used and the pellets were epoxied (0.2 mm of epoxy, Tra-Bond 816H01 from Tra-Con, Inc., loaded with silver powder) to two disk-shaped copper leads. The thermal conductivities were measured under vacuum of 10^{-4} Torr. The principles of operation for this technique are based on a pulse method.⁹ The geometry of the thermal conductivity sample was constrained in several ways. A pellet diameter of 4.74 mm was chosen so that the entire surface area would be covered by the QD copper lead (diameter of 6.30 mm). The thickness of the sample, ℓ , is limited by the thermal diffusion time constant for the sample defined by $\tau \sim C_P \times \ell^2 / \kappa$, where C_P is the heat capacity per unit volume and κ is the thermal conductivity. Too thick a sample would

^{a)} Author to whom correspondence should be addressed. Fax: 1 (902) 494-8016. Electronic mail: mary.anne.white@dal.ca

TABLE I. Size and density (at $T=300$ K) of HfMo_2O_8 pellets used for thermal conductivity measurements.

Sample	Thickness (mm)	Density (g cm^{-3})	% theoretical density
1	0.74	2.74	62.4
2	0.74	2.75	62.6
3	0.80	2.68	61.0
4	0.84	2.49	56.7
5	0.78	2.65	60.4

result in excessively long measurement times; the minimum thickness is governed by the optimal temperature drop across the sample ($\Delta T \sim 0.03T$). The maximum heater power P for the $2 \text{ k}\Omega$ heater in the PPMS is 50 mW , where $P = \kappa \Delta T (A/\ell)$ and A is the pellet's cross-sectional area. The optimal thickness for the pellets was approximately 0.8 mm . Thermal conductivities were measured using continuous methods, where measurements are taken continuously as the software adjusts parameters, such as the heater power and period, to optimize the measurements. The HfMo_2O_8 pellets were very fragile and many are fractured while the κ measurements were underway, as noted by a sudden drop in the apparent thermal conductivity. Often, the samples would break at the sample-epoxy interface, but in other instances, the pellet itself would fracture. In total, 27 samples were made to collect the data for HfMo_2O_8 ; details of the five pellets that gave useful data are given in Table I.

Figure 1 shows the temperature dependence of the thermal conductivity of HfMo_2O_8 for the samples measured. The uncertainties in κ were estimated from the accuracies in thermal conductance reported by the PPMS along with the uncertainties in the pellet dimensions [$\kappa = (K\ell)/A$, where K is the thermal conductance]. The overall uncertainty in the HfMo_2O_8 measurements is 20% for temperatures above 30 K but larger below 30 K.

The sample porosity ϕ , defined as $\phi = [100 \times [(\rho_{\text{bulk}} - \rho_{\text{eff}})/\rho_{\text{bulk}}] = 100 - (\% \text{ theoretical density})]$, can affect κ , and methods have been developed to estimate the correction for the porosity if the bulk κ is known,¹⁰ but it is not known for HfMo_2O_8 . Another method developed by Klemens¹¹ allows the calculation of the ratio of κ_{porous} to κ_{dense} directly from the porosity of the material,

$$\frac{\kappa_{\text{porous}}}{\kappa_{\text{dense}}} = 1 - \frac{4}{3}\phi, \quad (1)$$

for randomly oriented and randomly distributed voids. This approximation has been used recently by Schlichting *et al.* to

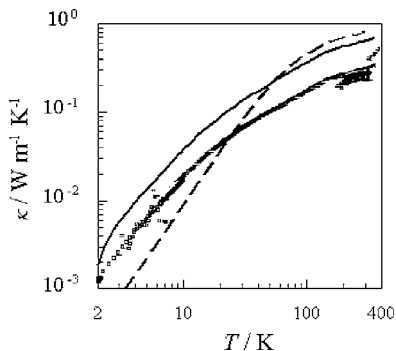


FIG. 1. Temperature dependence of thermal conductivity of HfMo_2O_8 pellets: (□) sample 1, (+) 2, (○) 3, (Δ) 4, (◇) 5, (—) κ_{dense} , and (---) κ_{min} .

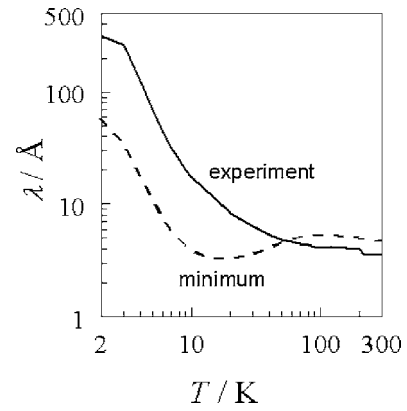


FIG. 2. Phonon mean free path of HfMo_2O_8 ; (—) from the κ_{dense} experimental thermal conductivity; (---) from the minimum thermal conductivity.

determine the effect of porosity in yttria-stabilized zirconia.¹² The values of κ_{dense} (for the average value of κ) of HfMo_2O_8 are shown as a function of temperature in Fig. 1. We find $\kappa_{\text{dense}} = 0.64 \pm 0.15 \text{ W m}^{-1} \text{ K}^{-1}$ at $T = 300 \text{ K}$ for HfMo_2O_8 .

As also found for ZrW_2O_8 , the present results indicate that HfMo_2O_8 does not exhibit the thermal conductivity temperature dependence of a “normal” (simple) crystalline solid. The thermal conductivities of both HfMo_2O_8 and ZrW_2O_8 are low, with positive temperature coefficients, $d\kappa/dT$, similar to the thermal conductivities of glasses,¹³ despite being crystalline materials.

In order to understand the low thermal conductivity, the theoretical minimum thermal conductivity κ_{min} of HfMo_2O_8 was calculated in Eq. (2) based on fully coupled oscillators for each of the transverse and longitudinal polarizations,¹³

$$\kappa_{\text{min}} = \frac{1}{2.48} k_B n^{2/3} v_i 2 \left(\frac{T}{\Theta_D^e} \right)^2 \int_0^{\Theta_D^e/T} \frac{x^3 e^x}{(e^x - 1)^2} dx, \quad (2)$$

where n is the number density of atoms per unit volume and the Debye characteristic temperature Θ_D^e is defined as

$$\Theta_D^e = \left(\frac{h}{2\pi k_B} \right) v_i (6\pi^2 n)^{1/3}, \quad (3)$$

i.e., treating all the lattice modes (in this case 3 acoustic and 129 optical) as Debye-like. From the heat capacity of HfMo_2O_8 ,^{14,15} we find $\Theta_D^e = 290 \text{ K}$ and a mean velocity of sound, v_i of 2900 m s^{-1} . The unit cell dimensions used for the calculation of molar volume were from the unit cell parameters at $T = 300 \text{ K}$ and the temperature-dependent thermal expansion coefficient.⁷ The experimental thermal conductivity of HfMo_2O_8 is very low (Fig. 1) and close to the theoretical minimum, as was also observed for ZrW_2O_8 .⁶

Using the experimental thermal conductivity data, the effective phonon mean free path λ was calculated in the Debye equation [Eq. (4)] for thermal conductivity,

$$\kappa = \frac{C v_i \lambda}{3}, \quad (4)$$

where C is the heat capacity per unit volume. (We refer to this as an *effective* mean free path because it generally underestimates the mean free path by comparison with a more accurate model that includes dispersion.¹⁶) The results are shown in Fig. 2. The effective mean free path at $T > 40 \text{ K}$ is approximately 10 \AA or less, on the same order as for non-crystalline materials such as amorphous SiO_2 despite the fact

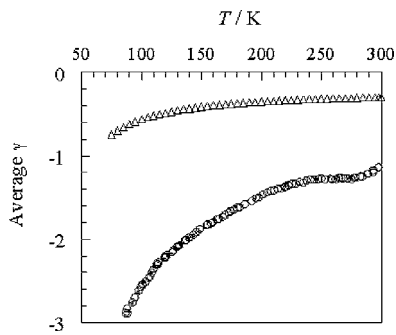


FIG. 3. Temperature dependence of the average Grüneisen function (Δ) HfMo_2O_8 and (\circ) ZrW_2O_8 .

that HfMo_2O_8 is crystalline. A similar result was found for ZrW_2O_8 .⁶ The effective mean free path is close to its theoretical minimum, especially for $T > 50$ K (Fig. 2), indicating highly coupled phonons and high thermal resistance.

Anharmonic terms in the phonon-phonon interactions are responsible for thermal resistance in insulating materials, and the degree of anharmonicity can be quantified through the average Grüneisen parameter γ , defined in terms of bulk properties of a cubic solid,

$$\gamma = \frac{3BV\alpha_l}{C_V}, \quad (5)$$

where B is the bulk modulus (=43 GPa for HfMo_2O_8) (Refs. 7 and 8), V is the molar volume,⁷ α_l is the linear thermal expansion coefficient,⁷ and C_V is the specific heat.^{14,15} The magnitudes of the average Grüneisen parameters for HfMo_2O_8 (Fig. 3) are rather large in comparison with other ceramics,¹ and the magnitude increases for $T < 150$ K, as for ZrW_2O_8 .⁶ Analyses of the contributions of various modes to the heat capacity of ZrW_2O_8 (Ref. 6) and HfMo_2O_8 (Ref. 15) indicate that for $T > 60$ K the modes below 10 meV, which are most relevant for negative thermal expansion,¹⁷⁻¹⁹ are essentially fully excited. From the calculation of γ , these modes are highly anharmonic, as γ deviates significantly from zero, as shown in Fig. 3. However, the values of γ for HfMo_2O_8 are of smaller magnitude than for ZrW_2O_8 , coinciding with the less negative thermal expansion coefficient. (HfW_2O_8 is intermediate in both γ (Ref. 20) and thermal expansion.²¹) The low-frequency optical modes are essentially fully coupled with the heat-carrying acoustic modes for

both HfMo_2O_8 and ZrW_2O_8 , leading to high resistance to heat flow, and low thermal conductivity. It is likely that low thermal conductivity is a general feature of this family of materials, intrinsically related to their negative thermal expansion.

The authors gratefully acknowledge financial support from NSERC, the Killam Trusts, and the Canada Foundation for Innovation, Atlantic Innovation Fund, and other partners that fund the Facilities for Materials Characterization managed by the Institute for Research in Materials. They would also like to thank M. Jakubinek and M. Stancescu for experimental assistance and C. Lind for helpful discussions. The work performed at the Georgia Institute of Technology was supported by the U.S. NSF through Grant Nos. DMR-0203342 and DMR-0605671.

- ¹G. D. Barrera, J. A. O. Bruno, T. H. K. Barron, and N. L. Allen, *J. Phys.: Condens. Matter* **17**, R217 (2005).
- ²A. W. Sleight, in *Thermal Conductivity* edited by R. B. Dinwiddie, M. A. White, and D. L. McElroy (DEStech, Lancaster, PA, 2006), Vol. 28, p. 131.
- ³C. Martinek and F. A. Hummel, *J. Am. Ceram. Soc.* **51**, 227 (1968).
- ⁴J. S. O. Evans, T. A. Mary, T. Vogt, M. A. Subramanian, and A. W. Sleight, *Chem. Mater.* **8**, 2809 (1996).
- ⁵T. A. Mary, J. S. O. Evans, T. Vogt, and A. W. Sleight, *Science* **272**, 90 (1996).
- ⁶C. A. Kennedy and M. A. White, *Solid State Commun.* **134**, 271 (2005).
- ⁷C. Lind, Ph.D. thesis, Georgia Institute of Technology, Athens, GA, 2001.
- ⁸C. Lind, D. G. VanDerveer, A. P. Wilkinson, J. Chen, M. T. Vaughan, and D. J. Weidner, *Chem. Mater.* **13**, 487 (2001).
- ⁹O. Maldonado, *Cryogenics* **32**, 908 (1992).
- ¹⁰V. V. Murashov and M. A. White, *J. Mater. Sci.* **35**, 649 (2000).
- ¹¹P. G. Klemens, *High Temp. - High Press.* **23**, 241 (1991).
- ¹²K. W. Schlichting, N. P. Padture, and P. G. Klemens, *J. Mater. Sci.* **36**, 3003 (2001).
- ¹³D. G. Cahill and R. O. Pohl, *Annu. Rev. Phys. Chem.* **39**, 93 (1988).
- ¹⁴C. A. Kennedy, Ph.D. dissertation, Dalhousie University, Halifax, NS, Canada, 2005.
- ¹⁵C. A. Kennedy, M. A. White, A. P. Wilkinson, and T. Varga (unpublished).
- ¹⁶G. Chen, *Int. J. Therm. Sci.* **39**, 471 (2000).
- ¹⁷G. Ernst, C. Broholm, G. R. Kowach, and A. P. Ramirez, *Nature (London)* **396**, 147 (1998).
- ¹⁸T. R. Ravindran, A. K. Arora, and T. A. Mary, *Phys. Rev. B* **67**, 064301 (2003).
- ¹⁹K. Wang and R. Reeber, *Appl. Phys. Lett.* **76**, 2203 (2000).
- ²⁰Y. Yamamura, N. Nakajima, T. Tsuji, Y. Iwasa, K. Saito, and M. Sorai, *Solid State Commun.* **121**, 213 (2002).
- ²¹Y. Yamamura, N. Nakajima, and T. Tsuji, *Phys. Rev. B* **64**, 184109 (2001).